Journal of Organometallic Chemistry, 454 (1993) 123–131

JOM 23498

New metallocene complexes of Nb and Ta with functionalized diazoalkanes

D.A. Lemenovskii, M. Putala, G.I. Nikonov and N.B. Kazennova
Chemical Department, Moscow State University, Moscow 118899 (Russian Federation)

D.S. Yufit and Yu.T. Struchkov
Institute of Organoelement Compounds, Russian Academy of Sciences, Moscow 117813 (Russian Federation)

(Received December 2, 1992)

Abstract

The reaction of Cp_2MH_3, where M ≡ Nb or Ta, with N_2CPh_2, $N_2CPh(o\text{-}C_6H_4Br)$ and $N_2CHCOOEt$ was thoroughly studied. It was shown that the primary products of the reaction are the complexes $Cp_2M(H)(\eta^1\text{-}N_2CRR')$ (**2**). The complexes **2** are readily oxidized by air to give polymeric $(Cp_2MO)_n$, N_2CRR' and $RR'CN_2CRR'$.

Interaction of an excess of $N_2CPh(o\text{-}C_6H_4Br)$ with Cp_2NbH_3 leads to a 17-electron complex $Cp_2Nb(-\overline{N\text{-}N{=}CPh\text{-}o\text{-}C}_6H_4)_2$ (**6**) with two σ-N pyrazole ligands. Finally the reaction of Cp_2NbH_3 with $N_2CHCOOEt$ gives an unusual dimeric complex $Cp_2Nb_2(\eta^5\text{-}C_5H_4C(COOEt){=}N\text{-}\mu\text{-}N)_2$. The complexes **2** were found to undergo easily substitution of a hydride ligand for a halogen atom.

The results of X-ray analysis of the complexes **6** and $Cp_2Nb(Cl)\text{-}\eta^1\text{-}N_2CPh(o\text{-}C_6H_4Br)$ are provided.

1. Introduction

Organic diazocompounds are highly reactive substrates having several reaction centres in one molecule. This makes them promising reagents for synthesis of functionalized organometallic complexes. With transition metal complexes, diazoalkanes were shown to give both addition products (the so-called "nitrene complexes" with various types of coordination of the nitrene ligand) and products of insertion of the diazoalkane into the M–L bond ("hydrazide complexes" also with various types of coordination of a hydrazide ligand). Because the total number of publications in this field is small, no rule describing the transformations that take place can be derived [1–4]. It is also necessary to take into consideration the fact that there are few examples of reactions of several transition metal complexes with diazoalkanes, resulting in dinitrogen elimination to produce carbene complexes [5–7].

The reactions of mononuclear polyhydride metal complexes with diazoalkanes have not been studied previously. We think, however, that just here the real opportunity arises to retrace the sequence of transformations of diazoalkane molecules in the coordination sphere of a transition metal. Hydride ligands are most mobile and one should expect no difficulties in the observation of the subsequently formed complexes. In this paper we report our study of reactions of dicyclopentadienyltrihydride compounds Cp_2MH_3 of Nb and Ta with some diazoalkane derivatives.

2. Results and discussion

We studied the reaction of trihydrides of niobocene and tantalocene, Cp_2MH_3, with three diazoalkanes: N_2CPh_2, $N_2CPh(o\text{-}C_6H_4Br)$ and $N_2CHCOOEt$. Various types of complex were isolated, depending on the reagent ratio, temperature and isolation procedure.

Correspondence to: Dr. D.A. Lemenovskii.

0022-328X/93/$6.00

Under moderate temperature conditions the first step of the process takes place, namely the reaction of ligand exchange:

$$Cp_2MH_3 + N_2CPhAr \longrightarrow$$

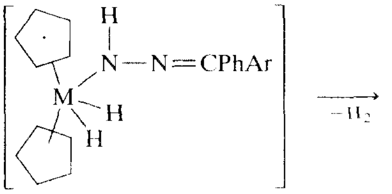

1a–c

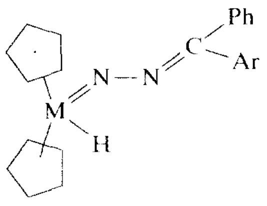

2a–2c

where M ≡ Nb, Ar ≡ Ph, in **1a** and **2a**, M ≡ Nb, Ar ≡ o-C_6H_4Br, in **1b** and **2b** and M ≡ Ta, Ar ≡ Ph, in **1c** and **2c**.

During the reaction a molecule of hydrogen is eliminated and the process yields almost quantitatively diamagnetic nitrene complexes **2a–2c** whose structures were derived from ^1H nuclear magnetic resonance (NMR) spectra and are confirmed with the results of X-ray analysis of Nb compounds.

The question on the mechanism of formation of **2a–2c** is of interest. We believe that the reaction proceeds via an intermediate **1**, the product of a direct insertion of the nitrene-like tip of diazoalkane molecule into the M–H bond. This seems quite reasonable for two reasons. The first reason is that the effective reaction rate of formation of **2a–2c** from the metallocenetrihydrides is much greater than the rate of a monomolecular thermolysis reaction of these trihydrides:

$$Cp_2MH_3 \longrightarrow [Cp_2MH] \longrightarrow Cp_2M_2(H)_2(\mu\text{-}C_5H_4)_2$$

This reaction is known to be very slow and it leads to bis-metallocene complexes. The second reason is that the insertion reaction of diazoalkanes into M–H bonds is not uncommon and it was observed for example in case of some Os [8] and Zr [4] compounds. As to the feasible route of transformation of the intermediate **1** into **2** we think that it will be helpful to formulate the following. Substitution of a hydrogen atom by the nitrogen atom transforms the bonding ψ orbital into ψ'; the contribution to ψ' from the residual hydride ligands is a maximum:

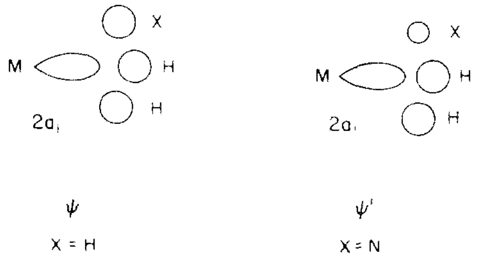

The contribution to the orbital ψ' from a hybrid orbital of the nitrogen is less than the corresponding value of a hydrogen atomic orbital because of the greater electronegativity of nitrogen atom. So substitution of an H atom for an N atom augments direct bonding H ··· H interaction between the residual hydride ligands in the coordination sphere of the central metal atom and promotes the further process of elimination of the H_2 molecule. In fact it is equivalent to an increase in the contribution of resonance structure B compared with that of the structure A in the complex **1**; it is structure B which is responsible for the process of H_2 molecule elimination:

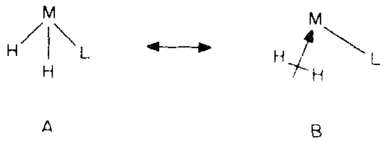

The H_2 elimination process in **1** generates the electron- and coordination-unsaturated intermediate **4**, which is rapidly rearranged into the stable complex **2** by the process of α-hydride shift:

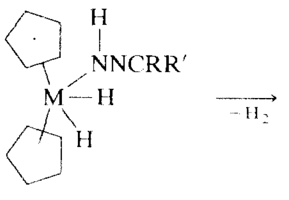

1

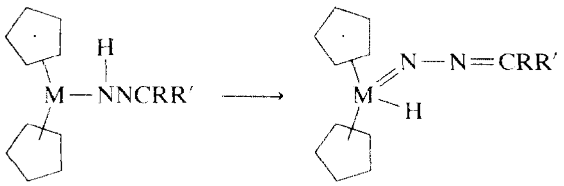

4 **2**

Such a shift is in a fact a well-known example of α elimination and it was observed for example in an isoelectronic cation molecule $Cp_2WCH_3^+$ [9].

The complexes **2a**–**2c** are orange crystalline solids stable in an inert atmosphere up to 80°C. In air they are slowly oxidized to give free diazoalkane derivative, ketazine **5**, and polymeric insoluble oxometallocene $(Cp_2MO)_n$:

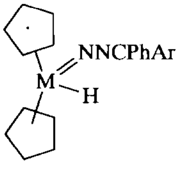

2

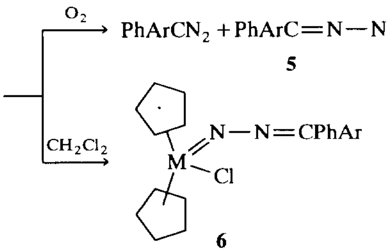

6

Formation of the free diazomethane derivative was revealed because of increase in the peak of free diazogroup, $\nu = 2040$ cm^{-1}, in the IR spectra of **2** in air. In the case of **2b** the corresponding ketazine **5b** was isolated as large yellow crystals whose structure was confirmed by X-ray analysis (Fig. 1), the details of which will be published later. We think that formation of **5b** may be accounted for in two ways. The first mechanism includes only organic molecules:

$$PhArCN_2 \xrightarrow[-N_2]{} [PhArC:] \xrightarrow{N_2CPhAr} PhArCNNCPhAr$$

5

The second mechanism supposes a direct attack of diazoalkane on the complex **2**:

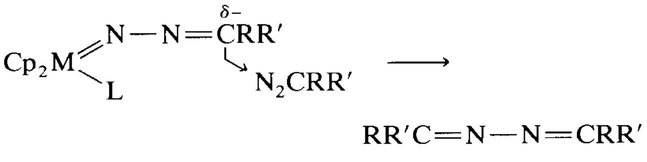

5

That is the methylene carbon atom in the diazoalkane ligand appears as a nucleophilic centre. A similar "umplung" of a reaction centre was observed earlier in the reaction of $(Cp_2ZrNNCPh_2)_2$ with ketones [10]. We isolated only one stereo isomer of **5b**, and we do not know whether other stereo isomers are formed, or the process of **5b** formation is very stereo selective by

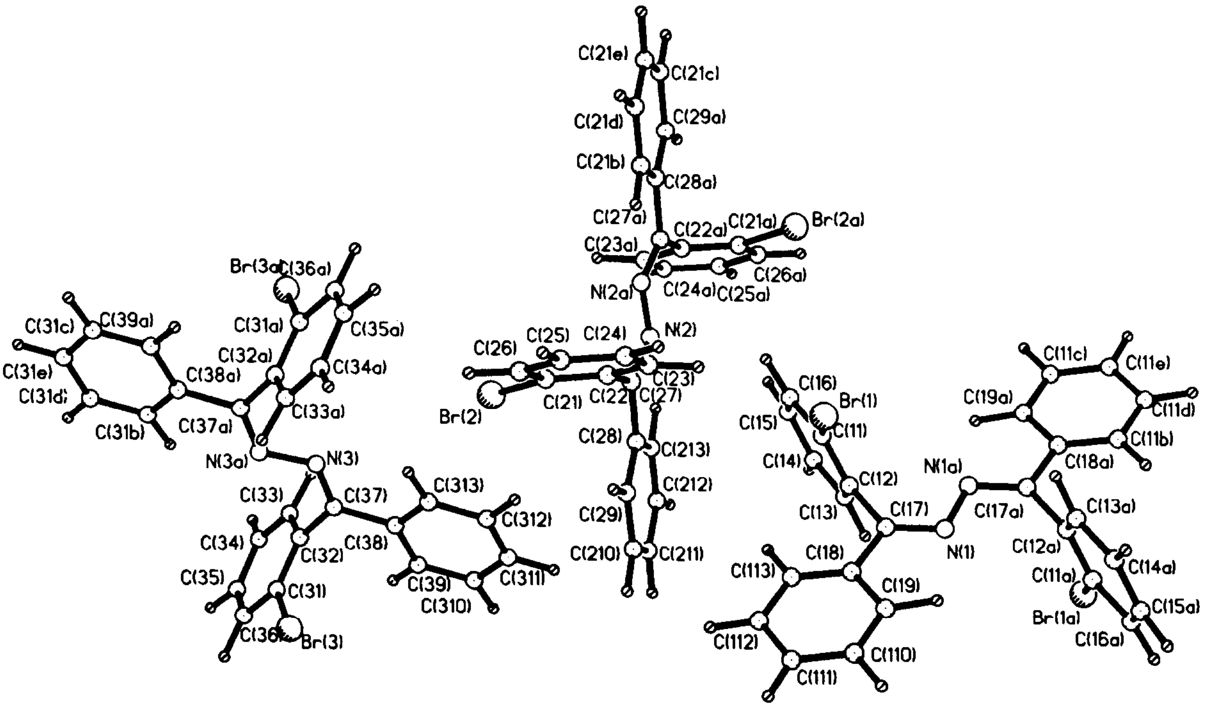

Fig. 1. Three independent molecules in the crystal structure of ketazine 5.

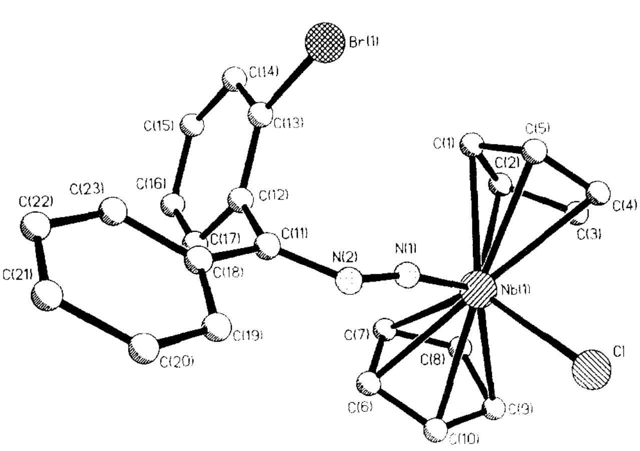

Fig. 2. The molecular structure of the complex **6**.

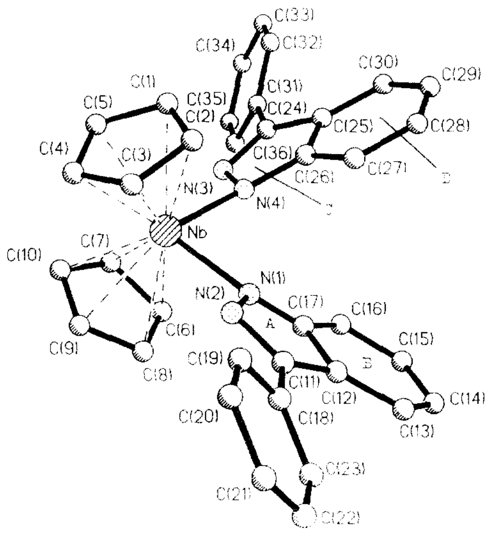

Fig. 3. The molecular structure of the complex **7**.

itself. The last proposition may be true if the second mechanism dominates.

Reaction of the hydrides **2a–2c** with halogenated solvents at room temperature smoothly results in quantitative exchange of the hydride ligand for a halogen. For one of the isolated complexes, $Cp_2Nb(Cl)N_2CPh(o\text{-}C_6H_4Br)$, single-crystal X-ray analysis was performed (Fig. 2).

We found two processes characteristic of transformation routes of the complexes of the type **2**. One of them was fulfilled when an excess of $N_2CPh(o\text{-}C_6H_4Br)$ was treated with Cp_2NbH_3 at moderate heating:

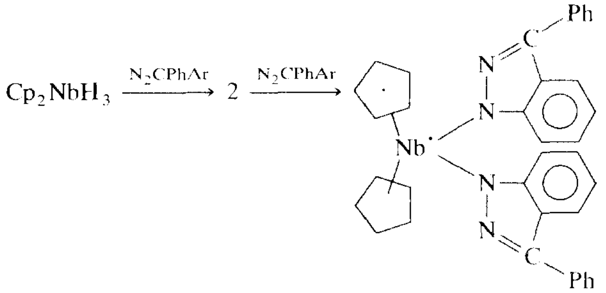

7

where Ar ≡ $o\text{-}C_6H_4Br$. This process results in the formation of new ligands of pyrazole type originating from the substitution reaction of the Br in $o\text{-}C_6H_4Br$ for the N atom. Two such ligands are bonded with Nb, giving rise to a 17-electron complex **7** with a d^1 configuration. The structure of **7** was revealed after an X-ray analysis study (see Fig. 3 later).

The second process was found to take place in the reaction of Cp_2NbH_3 with diazoacetic ester. In this case the process is not terminated on the step of formation of the complexes **2**. It proceeds more deeply to give the binuclear niobocene complex of a new type **8**:

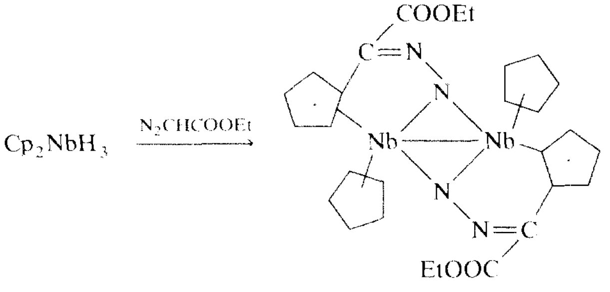

8

In this complex **8** both Nb atoms are connected with two bridging nitrene ligands. Insertion of the diazoalkane ligand in the cyclopentadienyl rings is a unique feature of the process and of the resulting complex. Nothing similar was ever observed when a complex organic molecule is added to a metallocene compound simultaneously in two places, by the central atom and to the cyclopentadienyl cycle. Detailed discussion of

TABLE 1. NMR ^1H spectra of $Cp_2M(X)(N_2CRR')$: **2a–2c** and **6** (in C_7D_8)

Complex	δ(Cp) (intensity)	δ(R, R′) [a] (intensity)	δ(M–H) [b] (intensity)
2a	5.165(10)	6.93–7.22(10)	1.27(1)
2b	5.139(10)	6.95–7.26(10)	1.22(1)
2c′ : **2c″** = 5 : 1; **2c′**	5.232(5); 5.233(5)	6.75–7.60(9)	1.25(1) [c]
(Two isomers) **2c″**	5.167(5); 5.165(5)		
6′ : **6″** = 4 : 3; **6′**	5.821(10)	6.75–7.60(9)	–
(Two isomers) **6″**	5.777(10)		

[a] Complex multiplets. [b] Broad signals. [c] Signal of the main isomer.

TABLE 2. Bond lengths (Å) in compound **6**

Nb–Cl	2.496(3)	C(2)–C(3)	1.35(3)
Nb–N(1)	1.84(1)	C(3)–C(4)	1.39(3)
Nb–C(1)	2.45(1)	C(4)–C(5)	1.46(2)
Nb–C(2)	2.48(2)	C(6)–C(7)	1.38(3)
Nb–C(3)	2.48(1)	C(6)–C(10)	1.38(2)
Nb–C(4)	2.43(2)	C(7)–C(8)	1.39(2)
Nb–C(5)	2.45(2)	C(8)–C(9)	1.35(3)
Nb–C(6)	2.43(1)	C(9)–C(10)	1.42(2)
Nb–C(7)	2.49(2)	C(11)–C(12)	1.52(1)
Nb–C(8)	2.49(2)	C(11)–C(18)	1.48(1)
Nb–C(9)	2.44(1)	C(18)–C(19)	1.35(2)
Nb–C(10)	2.41(2)	C(18)–C(23)	1.39(1)
Br–C(13)	1.863(6)	C(19)–C(20)	1.43(2)
N(1)–N(2)	1.29(1)	C(20)–C(21)	1.37(2)
N(2)–C(11)	1.30(2)	C(21)–C(22)	1.36(2)
C(1)–C(2)	1.39(2)	C(22)–C(23)	1.40(2)
C(1)–C(5)	1.34(3)		

this reaction and of the results of the structural study of the complex **8** will be published later.

Our results concerning the structure of the new diazoalkane complexes **2a**–**2c**, **6** and **8** positively refute the earlier supposition [12] that such compounds should contain η^2-(N–N) diazoalkane bonded ligands. As was shown, all the complexes without exception consist of η^1-N-coordinated N_2CRR' ligands.

2.1. ^1H nuclear magnetic resonance spectra of 2a–2c and 6

The ^1H NMR spectra of compounds **2a**–**2c** and **6** recorded at 300 K are given in Table 1. The spectra are very similar to each other, the signal of Cp and Ar protons being observed in their typical range. Only the situation of the signals of the M–H protons at $\delta = 1.2$ ppm is worth discussing. This differs significantly from the situation of the same M–H proton resonance signal in many other hydride complexes of the formula Cp_2MH_3 and $Cp_2M(L)H$, where M is Nb or Ta, and L can be a variety of ligands. Generally the above mentioned signals fall in the δ range from -2 to -10 ppm. We suppose that this significant down-field shift of the M–H proton resonance signals is due to anisotropic features of the M=N and N=N bonds and is regulated subtly by the bond lengths and the general geometry of the $\mathrm{H{-}M{=}N{=}N{=}C}$ fragments. The M–H proton resonance signal situation studied for **2a** is found to be temperature independent at least to 230 K (for **2a**, Nb–H; 1.27 ppm), but the width of the signal is substantially decreased. The cause for the signal width transformation is not evident but it is a fact of the experiment that there are no dynamic structural transformations with the complex **2a** in this temperature range.

Geometrical isomerism of the molecules **2c** and **6** gives rise to a double set of the resonance signals for each sample:

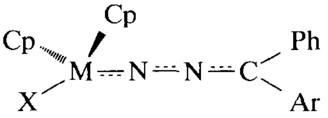

and

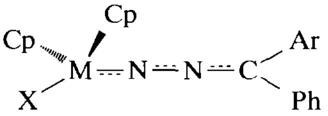

where X ≡ H, Cl.

From the structural data it is also evident (Fig. 2) that in the case when the Ar group is an asymmetrically substituted Ph, as in our *o*-C_6H_4Br-containing complex, hindrance of rotation about the C–C_6H_4Br bond in the NMR experiment time scale may result in magnetic non-equivalence of the Cp-ring protons. Such non-equivalence is observed for the isomers **2c′** and **2c″** but, in the case of the isomers of complex **6**, rotation by the C–C_6H_4Br bond is still free at room temperature.

2.2. The structure of $Cp_2Nb(Cl)N_2CPh(o\text{-}C_6H_4Br)$

The structure of $Cp_2Nb(Cl)N_2CPh(o\text{-}C_6H_4Br)$ (**6**) (Fig. 2 and Tables 2 and 3) is very similar to that reported for $Cp_2Nb(H)N_2CPh_2$ (**2a**) [11]. The Nb atom has a disordered tetrahedral coordination if all the ligands are regarded as monodentate. The bond lengths and angles are listed in Tables 2 and 3. The Nb–X bonds (X is the Cp-ligand d centroids) and mean C–C bond distances (2.15(2) and 1.39(3) Å) in the Cp rings are close to those found for the related complexes given in Table 4. Complex **6** has a Cl atom in place of an H atom in **2a** and the Nb–Cl bond length (2.496(3) Å) is elongated in comparison with that (2.470(5) Å

TABLE 3. Bond angles (°) in compound **6**

Cl–Nb–N(1)	92.3(3)	N(2)–C(11)–C(18)	119.6(8)
Nb–N(1)–N(2)	168.1(9)	C(12)–C(11)–C(18)	118.8(9)
N(1)–N(2)–C(11)	125.8(9)	C(11)–C(12)–C(13)	120.5(5)
C(2)–C(1)–C(5)	111.5(14)	C(11)–C(12)–C(17)	119.5(5)
C(1)–C(2)–C(3)	107.6(17)	Br–C(13)–C(12)	121.9(2)
C(2)–C(3)–C(4)	109.0(13)	Br–C(13)–C(14)	118.1(2)
C(3)–C(4)–C(5)	107.1(16)	C(11)–C(18)–C(19)	121.1(9)
C(1)–C(5)–C(4)	104.9(16)	C(11)–C(18)–C(23)	118.9(11)
C(7)–C(6)–C(10)	108.8(14)	C(19)–C(18)–C(23)	120.0(10)
C(6)–C(7)–C(8)	107.6(15)	C(18)–C(19)–C(20)	120.2(11)
C(7)–C(8)–C(9)	108.9(16)	C(19)–C(20)–C(21)	119.3(13)
C(8)–C(9)–C(10)	108.3(12)	C(20)–C(21)–C(22)	120.4(11)
C(6)–C(10)–C(9)	106.3(16)	C(21)–C(22)–C(23)	120.6(11)
N(2)–C(11)–C(12)	120.5(8)	C(18)–C(23)–C(22)	119.5(12)

TABLE 4. Structural parameters of some niobocenes of $Cp_2NbL'L''$ type

Compound	φ (°)	Mean C–C distance in Cp rings (Å)	θ (°)	Nb–C(Cp) distance (Å)	Reference
$Cp_2NbCl(N_2CPhC_6H_4Br)$	92.3(3)	1.39(3)	129.2	2.460(2)	This work
$Cp_2NbH(N_2CPh_2)$	94(2)	1.40(1)	134.9	2.440(7)	[11]
Cp_2NbCl_2	85		130.9 126.9		[13]
$Cp_2Nb(\overline{NNCPh\text{-}o\text{-}C_6H_4})_2$	88.9(3)	1.40(1)	131.1	2.400(1)	This work
$Cp_2Nb(CH_2Ph)_2$	79.0(4)	1.40(2)	133.1 133.2	2.410(26)	[22]
$Cp_2Nb(C_2H_5)(C_2H_4)$	–	1.363(7)	132.3	2.402(5)	[23]
$Cp_2Nb(C_3H_4)(CS_2)$	–		132.4 131.6		[24]

φ is the angle between L ligands in the bisector plane of the $Cp_2NbL'L''$ moiety and θ is the dihedral angle between the Cp planes.

[13]) in the Cp_2NbCl_2 structure. Cp rings are planar within 0.004 Å; the dihedral angle between their planes is $\theta = 129.2°$.

The geometry of the diazomethane moiety is also very similar to that found in other complexes containing terminal N_2CRR' ligands [14–19]: the N(1), N(2), C(N), C(12) and C(18) atoms are coplanar, and the NbN(1)N(2) angle significantly larger than 120° but noticeable smaller than 180° (168.1(9)° in **6**). The Nb–N distance of 1.84(1) Å (1.85 Å in **2a**) is shorter than that typical of a single Nb–N bond (2.135–2.23 Å; see discussion for **7** below). The N(1)–N(2) and N(2)–C(N) bonds (1.29 and 1.30 Å respectively) are elongated compared with the double N=N and C=N bonds (1.22 Å and 1.28 Å respectively [20]), being at the same time very close to corresponding parameters of **2a**. Thus it is possible to describe the N(2) bond geometry in sp^2 hybridization terms. The most appropriate description of the N(1) hybridization seems to be sp^x with $1 < x < 2$.

The alternative interpretation of bonding in the Nb–N–N–C fragment may involve the overlap of the N(1) hybrid σ orbital with the $2a_1$ and b_2 orbitals of the Cp_2Nb moiety (its symmetry is regarded as C_{2v}) [21], and the overlap of the N(1) π orbital in the bisector plane of the sandwich with the a_1 orbital of the Cp_2Nb:

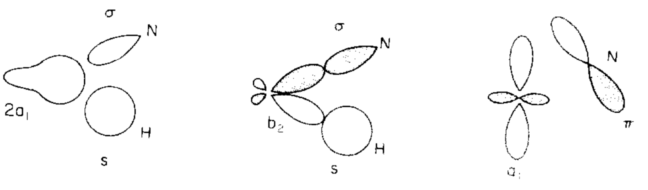

In this case the Nb–N bond order is a slightly less than the double bond, because the overlap of the π and a_1 orbitals is not very effective. The π orbitals of N(1), N(2) and C(N) atoms on the contrary overlap quite effectively and are orthogonal to the Cp_2 bisector plane. Thus the Nb–N–N system may regarded as a distorted "cumulene" fragment.

2.3. *The structure of $Cp_2Nb(N_2C_{13}H_9)_2$*

The molecular structure of **7** (Fig. 3) belongs to an extensively studied type of the Cp_2NbL_2 species. The Nb atom has tetrahedral coordination. The geometrical parameters of the niobium environment in **7** and related structures are shown in Table 4; the bond lengths and angles of **7** are given in Tables 5 and 6.

The most interesting feature is the structure of the ligand L which is a five-membered azine cycle conju-

TABLE 5. Bond lengths (Å) in compound 7

Nb–N(1)	2.188(8)	C(9)–C(10)	1.41(1)
Nb–N(4)	2.16(1)	C(11)–C(12)	1.45(2)
Nb–C(1)	2.45(2)	C(11)–C(18)	1.46(2)
Nb–C(2)	2.39(1)	C(12)–C(13)	1.41(2)
Nb–C(3)	2.36(2)	C(12)–C(17)	1.47(1)
Nb–C(4)	2.39(2)	C(13)–C(14)	1.38(2)
Nb–C(5)	2.41(1)	C(14)–C(15)	1.42(1)
Nb–C(6)	2.39(1)	C(15)–C(16)	1.40(2)
Nb–C(7)	2.37(1)	C(16)–C(17)	1.44(2)
Nb–C(8)	2.45(1)	C(18)–C(19)	1.38(2)
Nb–C(9)	2.43(1)	C(18)–C(23)	1.40(1)
Nb–C(10)	2.39(1)	C(19)–C(20)	1.39(2)
N(1)–N(2)	1.39(1)	C(20)–C(21)	1.39(2)
N(1)–C(17)	1.25(2)	C(21)–C(22)	1.37(2)
N(2)–C(11)	1.34(1)	C(23)–C(22)	1.37(2)
N(3)–N(4)	1.38(1)	C(24)–C(25)	1.43(1)
N(3)–C(24)	1.32(1)	C(24)–C(31)	1.51(1)
N(4)–C(26)	1.41(1)	C(25)–C(26)	1.42(2)
C(1)–C(2)	1.36(2)	C(25)–C(30)	1.41(2)
C(1)–C(5)	1.40(2)	C(26)–C(27)	1.43(1)
C(2)–C(3)	1.44(2)	C(27)–C(28)	1.37(2)
C(3)–C(4)	1.36(2)	C(28)–C(29)	1.42(2)
C(4)–C(5)	1.41(2)	C(29)–C(30)	1.38(1)
C(6)–C(7)	1.40(2)	C(31)–C(32)	1.37(2)
C(6)–C(8)	1.42(2)	C(31)–C(36)	1.39(2)
C(7)–C(10)	1.42(2)	C(32)–C(33)	1.39(2)
C(8)–C(9)	1.42(2)	C(34)–C(35)	1.37(2)
		C(34)–C(33)	1.39(2)
		C(35)–C(36)	1.38(1)

TABLE 6. Bond angles (°) in compound **7**

N(1)–Nb–N(4)	88.9(3)	N(1)–C(17)–C(16)	132.8(8)
Nb–N(1)–N(2)	112.1(8)	C(12)–C(17)–C(16)	115.6(12)
Nb–N(1)–C(17)	136.8(8)	C(11)–C(18)–C(19)	119.7(9)
N(2)–N(1)–C(17)	110.4(8)	C(11)–C(18)–C(23)	122.8(12)
N(1)–N(2)–C(11)	108.2(11)	C(19)–C(18)–C(23)	117.5(10)
N(4)–N(3)–C(24)	109.3(7)	C(18)–C(19)–C(20)	121.3(10)
Nb–N(4)–N(3)	117.7(7)	C(19)–C(20)–C(21)	119.5(15)
Nb–N(4)–C(26)	131.3(7)	C(20)–C(21)–C(22)	120.2(11)
N(3)–N(4)–C(26)	106.7(8)	C(18)–C(23)–C(22)	121.9(13)
C(2)–C(1)–C(5)	108.6(13)	N(3)–C(24)–C(25)	112.0(8)
C(1)–C(2)–C(3)	107.6(12)	N(3)–C(24)–C(31)	120.9(8)
C(2)–C(3)–C(4)	108.3(10)	C(25)–C(24)–C(31)	127.1(10)
C(3)–C(4)–C(5)	108.0(13)	C(24)–C(25)–C(26)	102.6(9)
C(1)–C(5)–C(4)	107.5(10)	C(24)–C(25)–C(30)	136.6(10)
C(7)–C(6)–C(8)	107.6(15)	C(26)–C(25)–C(30)	120.8(8)
C(6)–C(7)–C(10)	107.9(10)	N(4)–C(26)–C(25)	109.3(7)
C(6)–C(8)–C(9)	109.0(10)	C(25)–C(26)–C(27)	119.8(10)
C(8)–C(9)–C(10)	106.5(12)	C(26)–C(27)–C(28)	118.4(11)
C(7)–C(10)–C(9)	109.0(13)	C(27)–C(28)–C(29)	121.3(9)
N(2)–C(11)–C(12)	109.0(9)	C(28)–C(29)–C(30)	121.5(12)
N(2)–C(11)–C(18)	120.8(13)	C(25)–C(30)–C(29)	118.3(11)
C(12)–C(11)–C(18)	130.2(10)	C(24)–C(31)–C(32)	120.5(10)
C(11)–C(12)–C(13)	136.1(9)	C(24)–C(31)–C(36)	120.4(9)
C(11)–C(12)–C(17)	100.8(10)	C(32)–C(31)–C(36)	119.0(9)
C(13)–C(12)–C(17)	123.1(13)	C(31)–C(32)–C(33)	119.6(11)
C(12)–C(13)–C(14)	118.4(9)	C(35)–C(34)–C(33)	119.0(10)
C(13)–C(14)–C(15)	120.8(13)	C(34)–C(35)–C(36)	120.1(11)
C(14)–C(15)–C(16)	121.4(14)	C(31)–C(36)–C(35)	121.1(10)
C(15)–C(16)–C(17)	120.7(9)	C(21)–C(22)–C(23)	119.7(10)
N(1)–C(17)–C(12)	111.5(11)	C(32)–C(33)–C(34)	121.2(10)
N(4)–C(26)–C(27)	130.7(10)		

gated to benzene ring and connected with the metal through nitrogen.

The dihedral angles between planes of the five- and six-membered cycles are equal to 3.1° for A and B and 3.7° for C and D rings and the number of π electrons in the ligands L is 10. Therefore each ligand L in fact forms a common aromatic Huckel system. However, the N(1)–N(2) distance of 1.39(1) Å and the N(3)–N(4) distance of 1.38(1) Å indicate the low N–N bond order (the standard length of the N=N and N(sp^2)–N(sp^2) bonds are equal to 1.240 Å and 1.401 Å respectively [20]). Besides this the Nb–N distances of 2.188(8) and 2.16(1) Å are the same as in the complexes with single Nb–N(sp^2) bonds (2.18–2.23 Å [25] and 2.135 Å [26]). Moreover the coordination of the aromatic N atom with Nb (by the lone pair) is known to increase the Nb–N bond length (in phenanthroline, 2.307–2.321 Å [27], 2.318 Å [26] and 2.32–2.35 Å [28]).

The facts mentioned above indicate the disappearance of heterocycle aromaticity possibly related to the partial electron density transfer from the conjugated π system to the non-bonded a_1 orbital of the Cp_2Nb moiety [21]. This interaction may be realized in **7** because of the rotation of the ligand planes relative to the Cp rings bisector plane by about 27°. The rotation is the result of steric repulsion of ligands L in the coordination sphere of the Nb atom (C(16)–C(27), 3.26(2) Å).

3. Experimental details

All syntheses, isolation and purification of the products were carried out in sealed evacuated Schlenk-type vessels. All the solvents were thoroughly free from water and oxygen. NMR spectra were registered on a VXR 400 Varian instrument; IR spectra were recorded on a IKS-29 spectrometer (St. Petersburg Optical and Mechanical Works).

3.1. Syntheses of the new complexes

*3.1.1. Complex **2c***

To a red–violet solution of 2.35 g (8.6 mmol) of freshly purified $N_2CPh(o\text{-}C_6H_4Br)$ in 80 ml of toluene at 0°C, 1.83 g (8.09 mmol) of solid Cp_2NbH_3 were added. During a time of about 8 h the colour slowly turns deep red and hydrogen is evolved. The mixture is kept for another 12 h at room temperature. Then toluene is removed in vacuum and the solid residue is washed three times with portions of 10 ml ether to remove an excess of $N_2CPh(C_6H_4Br)$. The solid product is recrystallized from toluene. The yield of **2c** is 50–55% of the theoretical yield. Decomposition occurs above 80°C.

Found: C, 56.36; H, 4.54; Nb, 18.08. $C_{23}H_{20}NbN_2Br$ calc.: C, 55.56; H, 4.05; Nb, 18.68%.

From the starting solution small amounts, 5–7% yield, of **7** may be isolated.

*3.1.2. Complex **7***

Complex **7** is formed in tractable amounts in the synthesis similar to the above, provided that a twofold excess of $N_2CPh(C_6H_4Br)$ is used. After the first slow step is completed in about 8 h, the reaction mixture is heated to 50°C for 4 h and then it is kept for 10–12 h in a refrigerator at −5°C. The crystalline material precipitated on the walls of the reaction vessel is collected and dried. The yield of **7** is about 20%.

Found: C, 70.12; H, 4.25. $C_{36}H_{28}N_4Nb$ calc.: C, 70.93; H, 4.63%.

*3.1.3. Complex **6***

(0.100 g (0.2 mmol) of complex **2c** is dissolved in 5 ml of dry CH_2Cl_2. The solution is kept at room temperature for 24 h. During this time the colour changes from red to orange. After 24 h, 30 ml of pentane is condensed into the vessel, to allow slow mixing of the two phases by diffusion. Large crystals formed on the walls of the vessel are collected. The yield of **6** is 0.085 g, 83% of the theoretical value.

Found: C, 52.28; H, 4.02; Nb, 16.80. $C_{23}H_{19}N_2BrCl$-Nb calc.: C, 51.95; H, 3.60; Nb, 17.47%.

3.1.4. Complex 8

To a solution of 0.57 g (5.0 mmol) of $N_2CHCOOEt$ in 20 ml of toluene, 1.0 g (4.4 mmol) of Cp_2NbH_3 is added at room temperature. Slow evolution of H_2 is observed and the colour of the solution turned during 5–6 h to orange–brown. The mixture is kept for 12 h at room temperature and then for 5 h at 0°C. After the gaseous phase has been removed, the mixture is kept at −5°C for one night. The crystalline precipitate is decanted and recrystallized in vacuum from tetrahydrofuran. The yield of **8** is 0.2 g, 67% of the theoretical value.

Found: C, 50.23; H, 4.20; N, 8.34. $C_{28}H_{28}N_4O_4Nb_2$ calc.: C, 50.97; H, 4.53; N, 8.47%.

3.2. X-ray study

X-ray experiments were carried out with graphite-monochromated Mo Kα radiation (λ = 0.71069 Å) on a four-circle Syntex P2_1 diffractometer at 80°C for **6** and on a Siemens P3/PC diffractometer at −130°C for **7**. The θ–2θ scan mode was used in both cases. Anomalous scattering corrections were not included. All calculations were performed with the SHELXTL (PC

TABLE 7. Atom coordinates ($\times 10^4$) and temperature factors (Å^2 $\times$ 10^3) in compound **6**

Atom	x	y	z	U_{eq} [a]
Nb	2070(1)	7921(1)	3975(1)	28(1)
Cl	−266(2)	7992(2)	3443(2)	38(1)
Br	3481(2)	6719(1)	1124(1)	65(1)
N(1)	1916(9)	8185(7)	2522(7)	36(2)
N(2)	1778(8)	8531(7)	1565(7)	34(2)
C(1)	1871(15)	9414(9)	4525(12)	59(3)
C(2)	2036(16)	8917(9)	5481(11)	61(3)
C(3)	3219(17)	8584(11)	5860(11)	78(3)
C(4)	3801(16)	8842(11)	5140(16)	94(3)
C(5)	2906(17)	9401(10)	4277(14)	75(3)
C(6)	2037(16)	6422(9)	3395(14)	67(3)
C(7)	1475(14)	6401(9)	4175(15)	66(3)
C(8)	2390(16)	6629(10)	5226(13)	65(3)
C(9)	3486(15)	6792(9)	5104(11)	65(3)
C(10)	3293(14)	6659(9)	3945(13)	59(3)
C(11)	2680(9)	8672(7)	1200(8)	25(2)
C(12)	4055(5)	8457(4)	1923(5)	30(2)
C(13)	4512(5)	7617(4)	1948(5)	41(3)
C(14)	5777(5)	7430(4)	2603(5)	54(3)
C(15)	6583(5)	8084(4)	3233(5)	51(3)
C(16)	6126(5)	8924(4)	3207(5)	61(3)
C(17)	4862(5)	9110(4)	2552(5)	59(3)
C(18)	2380(9)	9095(7)	87(8)	25(2)
C(19)	3248(11)	9141(8)	−391(10)	42(3)
C(20)	2939(12)	9554(8)	−1464(9)	40(3)
C(21)	1770(12)	9926(8)	−1988(9)	38(3)
C(22)	898(12)	9875(8)	−1512(9)	38(3)
C(23)	1189(10)	9461(7)	−463(9)	32(3)

[a] The equivalent isotropic temperature factor U_{eq} defined as one third of the trace of the orthogonalized U_{ij} tensor.

TABLE 8. Atom coordinates ($\times 10^4$) and temperature factors (Å^2 $\times$ 10^3) in compound **7**

Atom	x	y	z	U_{eq} [a]
Nb	−471	1863	2820	27(1)
N(1)	−1494(10)	4126(10)	2066(4)	26(5)
N(2)	−2895(11)	4560(9)	1726(4)	37(5)
N(3)	2872(10)	669(9)	3206(4)	35(5)
N(4)	1714(9)	1621(9)	2650(4)	30(5)
C(1)	639(16)	−171(15)	2176(8)	52(8)
C(2)	−536(18)	1066(14)	1722(6)	47(8)
C(3)	−1882(15)	1338(13)	2059(7)	47(7)
C(4)	−1494(15)	276(13)	2712(7)	50(7)
C(5)	88(15)	−657(13)	2810(6)	42(8)
C(6)	−125(15)	2802(14)	3818(6)	45(8)
C(7)	306(14)	1268(13)	4096(5)	36(7)
C(8)	−1698(15)	3610(13)	3605(5)	40(7)
C(9)	−2242(13)	2569(13)	3729(5)	37(7)
C(10)	−997(15)	1128(13)	4045(5)	41(7)
C(11)	−3525(13)	6018(12)	1354(5)	31(6)
C(12)	−2476(12)	6553(11)	1423(5)	29(6)
C(13)	−2427(14)	7900(12)	1127(5)	37(6)
C(14)	−1177(14)	7969(12)	1340(6)	41(7)
C(15)	41(13)	6707(13)	1832(6)	40(7)
C(16)	19(13)	5360(12)	2119(5)	35(7)
C(17)	−1247(12)	5213(13)	1926(5)	22(6)
C(18)	−5038(11)	6812(11)	960(5)	25(6)
C(19)	−5601(12)	5996(12)	720(5)	36(6)
C(20)	−7056(14)	6702(13)	374(6)	52(7)
C(21)	−7966(12)	8264(14)	262(6)	45(7)
C(23)	−5993(12)	8384(11)	838(5)	28(6)
C(24)	4173(11)	269(11)	2932(5)	30(6)
C(25)	3973(12)	970(10)	2163(5)	19(6)
C(26)	2382(13)	1790(11)	1996(5)	30(6)
C(27)	1717(13)	2690(11)	1260(6)	36(6)
C(28)	2650(16)	2759(12)	739(6)	45(8)
C(29)	4243(15)	1939(13)	916(6)	44(7)
C(30)	4912(13)	1050(11)	1615(6)	35(6)
C(31)	5641(13)	−757(13)	3423(6)	36(7)
C(32)	6827(13)	−1882(12)	3183(6)	38(6)
C(34)	8364(14)	−2598(13)	4336(6)	46(7)
C(35)	7174(13)	−1475(13)	4572(6)	39(6)
C(36)	5816(12)	−575(12)	4126(6)	36(6)
C(22)	−7430(13)	9096(13)	498(6)	37(7)
C(33)	8189(13)	−2793(12)	3638(7)	40(7)
C(1′)	4014(15)	6176(16)	3225(8)	70(4)
C(2′)	3163(18)	4471(19)	3917(10)	93(5)
C(5′)	3461(23)	5861(24)	4003(11)	30(6)
C(6′)	3209(24)	6617(24)	4522(12)	153(8)
C(11′)	3474(28)	3892(29)	3416(15)	55(7)
C(12′)	3017(30)	5122(32)	4310(15)	61(8)
C(14′)	3865(30)	6641(30)	3722(15)	64(8)
C(15′)	3927(26)	4256(27)	2761(13)	153(9)
C(16′)	4137(24)	5532(25)	2759(12)	38(6)
C(17′)	3700(36)	4836(40)	3127(19)	83(10)

[a] The equivalent isotropic temperature factor U_{eq} is defined as one third of the trace of the orthogonalized U_{ij} tensor. Primed atoms were not refined.

version) program package. Both structures were solved by the direct method and refined using the full-matrix least-squares technique.

3.2.1. $Cp_2Nb(Cl)N_2CPh(C_6H_4Br\text{-}o)$ (6)

The red–orange crystals **6** were obtained by slow precipitation from CH_2Cl_2 solution on the addition of ether. The crystals **6** are monoclinic, of space group $P2_1/n$, with $a = 11.454(4)$ Å, $b = 15.448(7)$ Å, $c = 12.766(4)$ Å, $\beta = 112.67(3)°$, $V = 2084.3(2.8)$ Å^3, $d_{calc} = 1.694$ g cm^{-3}, $\mu = 25.92$ cm^{-1} and $Z = 4$. 2688 independent reflections with $I \geqslant 2\sigma(I)$ were measured to $(\sin\theta)/\lambda = 0.650$. All non-hydrogen atoms were refined anisotropically; all H atoms were placed in calculated positions and included in the refinement in the isotropic approximation. The C(12)–C(17) Ph ring was refined as a rigid group. The final discrepancy factors are $R = 0.080$ ($R_w = 0.087$); the atomic coordinates are listed in Table 7. The bond lengths and bond angles are listed in Tables 2 and 3 respectively.

3.2.2. $Cp_2Nb(N_2C_{13}H_9)_2$ (7)

The dark-red (almost black) crystals of **7** were grown directly in the reaction vessel. Crystals **7** are triclinic, of space group $P1$, with $a = 10.243(3)$ Å, $b = 10.423(3)$ Å, $c = 18.698(5)$ Å, $\alpha = 77.07(2)$; $\beta = 89.40(2)°$, $\gamma = 60.89(1)°$, $V = 1688.5(1.2)$ Å^3, $d_{calc} = 1.694$ g cm^{-3}, $\mu = 3.76$ cm^{-1} and $Z = 2$. Final atomic coordinates are given in Table 8. All non-hydrogen atoms were refined anisotropically; all hydrogen atoms were determined isotropically (most were located from the difference Fourier map; the remaining were placed in calculated positions). The structure was refined to $R = 0.059$ ($R_w = 0.059$) using 2167 reflections with $I > 2\sigma(I)$ and $(\sin\theta)/\lambda < 0.595$. The solvate toluene molecule in crystal **7** was found to be disordered over two positions; both of them were refined isotropically with equal site occupation factors G of 0.5. The bond lengths and bond angles are listed in Tables 5 and 6 respectively.

References

1 L.B. Kool, M.D. Rausch, H.G. Alt, M. Herberhold, A.F. Hill, U. Thewalt and B. Wolf, *J. Chem. Soc., Chem. Commun.*, (1986) 408.
2 S. Gambarotta, C. Floriani, A. Chiesi-Villa and C. Guastini, *J. Am. Chem. Soc., 105* (1983) 7295.
3 M.D. Curtis, L. Messerle, J.J. D'Errico, W.M. Butler and M.S. Hay, *Organometallics, 5* (1986) 2283.
4 S. Gambarotta, M. Basso-Bert, C. Floriani and C. Guastini, *J. Chem. Soc., Chem. Commun.*, (1982) 374.
5 A.D. Clauss, P.A. Dimas and J.R. Shapley, *J. Organomet. Chem., 201* (1980) C31.
6 L. Messerle and M.D. Curtis, *J. Am. Chem. Soc., 102* (1980) 7789.
7 N.M. Boag, M. Green, R.M. Mills, G.N. Pain, F.G.A. Stone and P. Woodward, *J. Chem. Soc., Chem. Commun.*, (1980) 1171.
8 M.R. Churchill and H.J. Wasserman, *Inorg. Chem., 20* (1981) 2905.
9 N.J. Cooper and M.L.H. Green, *J. Chem. Soc., Dalton Trans.*, (1979) 1121.
10 G.M. Arvasntis, J. Schwatz and D. Van Engen, *Organometallics, 5* (1986) 2157.
11 D.A. Lemenovskii, M. Putala, G.I. Nikonov, A.I. Zinin, N.B. Kazennova, A.S. Batsanov and Yu.T. Struchkov, *J. Organomet. Chem., 452* (1993) 87.
12 J.F. Leboeuf, J.C. Leblanc and C. Moise, *J. Organomet. Chem., 364* (1989) C22.
13 K. Prout, T.S. Cameron, R.A. Forder, S.R. Critchley, B. Denton and G.V. Ress, *Acta Crystallogr. B, 30* (1974) 2290.
14 K.D. Schramm and J.A. Ibers, *J. Am. Chem. Soc., 100* (1978) 2932.
15 M. Hidai, Y. Mizobe, M. Sago, T. Kodama and Y. Uchida, *J. Am. Chem. Soc., 100* (1978) 5740.
16 M.H. Chisholm, K. Folting, J.C. Huffman and A.L. Ratermann, *Inorg. Chem., 23* (1984) 2303.
17 R. Ben-Shoshan, J. Chatt, G.J. Leigh and W. Hussain, *J. Chem. Soc., Dalton Trans.*, (1980) 771.
18 M.J. Menu, G. Crocco, M. Dartiguenave, Y. Dartiguenave and G. Bertrand, *J. Chem. Soc., Chem. Commun.*, (1988) 1598.
19 D.L. Hughes, I.A. Latham and G.J. Leigh, *J. Chem. Soc., Dalton Trans.*, (1986) 393.
20 F.H. Allen, O. Kennard, D.G. Watson, L. Brammer, A.G. Orpen and R. Taylor, *J. Chem. Soc., Perkin Trans. II*, (1987) S1.
21 J. W. Lauher and R. Hoffmann, *J. Am. Chem. Soc., 98* (1976) 1729.
22 P.B. Hitchcock, M.F. Lappert and C.R.C. Milne, *J. Chem. Soc., Dalton Trans.*, (1981) 180.
23 L.J. Guggenberger, P. Meakin and F.N. Tebbe, *J. Am. Chem. Soc., 96* (1974) 5420.
24 M.G.B. Drew and L.S. Pu, *Acta Crystallogr. B, 33* (1977) 1207.
25 M.G.B. Drew and J.D. Wilkins, *J. Chem. Soc., Dalton Trans.*, (1974) 198.
26 E.J. Peterson, R.B. Von Dreele and T.M. Brown, *Inorg. Chem., 15* (1976) 309.
27 G. Mathern and R. Weiss, *Acta Crystallogr. B, 27* (1971) 1582.
28 B. Kamenar and C.K. Prout, *J. Chem. Soc. A*, (1970) 2379.